THE JOURNAL OF BIOLOGICAL CHEMISTRY
Vol. 277, No. 48, Issue of November 29, pp. 46110–46115, 2002
Printed in U.S.A.

Dual Effects of an Extra Disulfide Bond on the Activity and Stability of a Cold-adapted α-Amylase*

Received for publication, July 19, 2002, and in revised form, September 19, 2002
Published, JBC Papers in Press, September 24, 2002, DOI 10.1074/jbc.M207253200

Salvino D'Amico, Charles Gerday, and Georges Feller‡

From the Laboratory of Biochemistry, Institute of Chemistry B6, University of Liège, Liège 4000, Belgium

Chloride-dependent α-amylases constitute a well conserved family of enzymes thereby allowing investigation of the characteristics of each member to understand, for example, relevant properties required for environmental adaptation. In this context, we have constructed a double mutant (Q58C/A99C) of the cold-active and heat-labile α-amylase from the Antarctic bacterium *Pseudoalteromonas haloplanktis*, defined on the basis of its strong similarity with the mesophilic enzyme from pig pancreas. This mutant was characterized to understand the role of an extra disulfide bond specific to warm-blooded animals and located near the entrance of the catalytic cleft. We show that the catalytic parameters of the mutant are drastically modified and similar to those of the mesophilic enzyme. Calorimetric studies demonstrated that the mutant is globally stabilized ($\Delta\Delta G$ = 1.87 kcal/mol at 20 °C) when compared with the wild-type enzyme, although the melting point (T_m) was not increased. Moreover, fluorescence quenching experiments indicate a more compact structure for the mutated α-amylase. However, the strain imposed on the active site architecture induces a 2-fold higher thermal inactivation rate at 45 °C as well as the appearance of a less stable calorimetric domain. It is concluded that stabilization by the extra disulfide bond arises from an enthalpy-entropy compensation effect favoring the enthalpic contribution.

Disulfide bonds have attracted attention for many years, in particular as a possible means of studying the folding pathway and the stability of proteins. In 1988, Pace and coworkers (1) showed that disulfide bond removal decreases the stability of a protein principally by increasing the flexibility and conformational entropy of the unfolded state (chain entropy model). They proposed an equation to predict the effect of a cross-link on the conformational entropy of a protein: $\Delta S_{conf} = -2.1 - (1.5R \ln n)$, where R is the gas constant and n the number of residues between the side chains that are cross-linked. Doig and Williams (2) added in their analysis the contribution of the hydrophobic effect, as the main driving force in protein folding. They reached the opposite conclusion that cross-links surprisingly destabilize folded structures entropically but stabilize them enthalpically to a greater extent. They concluded that the stabilizing conformational entropy effect on the unfolded state is outweighed by the destabilizing effect the cross-link exercises by decreasing the amount of water ordered in the unfolded state. In contrast, the cross-link destabilizes the unfolded state enthalpically by inducing less favorable hydrogen bond networks as compared with an unconstrained random coil.

These studies have only considered the destabilizing effect of disulfide bonds on the unfolded state of a protein. Nevertheless, it seems clear that entropic and enthalpic effects on the native state must be considered as well (3). Introducing disulfide bridges can induce a potential destabilizing constraint on the native state, larger than the destabilizing effects on the denatured state, therefore, explaining why previous attempts in stabilizing proteins have not always been successful. Disulfide mutants of barnase have been extensively characterized by various biophysical methods and x-ray crystallography (4, 5). It was found that disulfide bonds could stabilize or destabilize local structures and therefore influence the global stability of the enzyme. Unfolding thermodynamics of barnase mutants (6) showed that the subtle balance of intramolecular and solvation contributions in both the native and unfolded states impairs a reliable predictability of thermodynamic changes. In other words, each cross-link, artificial or not, has properties that depend on the specific site occupied within the overall structure of the protein. Other studies have also shown that (i) the nature of individual amino acid residues introduced in disulfide removal can significantly modify the stabilization enthalpic term in both senses (7), (ii) cross-links stabilize both native and unfolded states, the difference causing either loss or gain in protein stability, (iii) enthalpy-entropy compensation accompanies disulfide bond effects, and (iv) protein stabilization depends on altered hydrophobicity of both native and unfolded states, altered flexibility near the cross-link, and residual structure in the unfolded state (8). All these studies reflect the huge diversity of ways by which a single cross-link can affect the thermodynamic parameters of a particular enzyme.

The cold-active and heat-labile α-amylase from the Antarctic bacterium *Pseudoalteromonas haloplanktis* (AHA)[1] is a chloride and calcium-dependent enzyme that hydrolyzes starch and related oligo- and polysaccharides. Chloride-dependent α-amylases are specific to all animals and some Gram-negative bacteria (9). This enzyme family displays a high percentage of sequence isology and structural similarity among all its members, thus allowing fine comparisons, at the molecular level, of enzymes adapted to different living environments. As a rule, cold-active or psychrophilic enzymes display a high catalytic efficiency to cope with the reduction in chemical reaction rates induced by low temperatures (10–12). This activity is, however,

* This work was supported by the European Union (CT970131), the Région Wallonne (Bioval 981/3860, Bioval 981/3848, Initiative 114705), the Fonds National de la Recherche Scientifique (FNRS) Belgium (Grant 2.4515.00), and the Institut Polaire Français. The costs of publication of this article were defrayed in part by the payment of page charges. This article must therefore be hereby marked "*advertisement*" in accordance with 18 U.S.C. Section 1734 solely to indicate this fact.

‡ To whom correspondence should be addressed. Tel.: 32-4-366-3389; Fax: 32-4-366-3364; E-mail: sdamico@ulg.ac.be.

[1] The abbreviations used are: AHA, *P. haloplanktis* α-amylase; PPA, pig pancreatic α-amylase; MutCC, double mutant Q58C/A99C from *P. haloplanktis* α-amylase; DSC, differential scanning calorimetry; ITC, isothermal titration calorimetry.

associated with a low thermal stability. In most cases, cold-adaptation is achieved through a reduction in the activation energy of the reaction that possibly originates from an increased flexibility of either a part or the overall protein structure (13). An extensive thermodynamic study of AHA has been carried out previously (14). AHA is the largest known protein undergoing a fully reversible thermal unfolding according to a two-state reaction pathway (15). It was proposed that its improved plasticity has led to this enzyme being close to the lowest possible stability allowing maintenance of the native conformation. Structural investigations have suggested that cold-adaptation was achieved by decreasing the number and strength of weak interactions stabilizing the native conformation (16, 17). This was confirmed by the calorimetric characterization of mutants from AHA defined on the basis of its strong similarity with the mesophilic α-amylase from the pig pancreas (PPA) (18).

Here, we report the characterization of the double mutant of AHA, MutCC (Q58C/A99C), introducing an extra disulfide bond. Our multiple sequence alignment of chloride-dependent α-amylases (9) revealed that four disulfide bonds are strictly conserved while one (C58–C99, AHA numbering) is specific to the enzymes from mammals and birds. Our goal was to investigate the importance of this cross-link (i) in the context of the thermal adaptation of these enzymes and (ii) to understand the role of disulfides in the stability, activity, and flexibility of proteins in general, and we show that many characteristics of MutCC are intermediate between AHA and PPA.

EXPERIMENTAL PROCEDURES

Mutagenesis and Protein Purification—Mutations in the *P. haloplanktis* α-amylase gene were introduced by PCR as described previously (19). The nucleotide sequence of the constructions was checked on an Amersham Biosciences ALF DNA sequencer. The recombinant wild-type α-amylase and the mutant enzyme were expressed in *Escherichia coli* at 18 °C and purified by DEAE-agarose, Sephadex G100, and Ultrogel AcA54 column chromatography, as previously described (20). Pig pancreatic α-amylase (PPA) was from Roche Molecular Biochemicals.

Enzyme Assay and Kinetics—The k_{cat} values were determined at 25 °C using 3.5 mM 4-nitrophenyl-α-D-maltoheptaoside-4,6-*O*-ethylidene as substrate (19). The k_{cat}/K_m values for substrate hydrolysis were determined from initial rates using the following relation: $k_{cat}/K_m = v_0/S_0E_0$, which is valid at $S_0 \ll K_m$ for systems that obey Michaelis-Menten kinetics. The validity of this equation was ascertained by performing determinations at three substrate concentrations.

Activation Parameters—The specific activities measured between 5 and 25 °C for AHA, PPA, and MutCC were used to construct Arrhenius plots (ln k_{cat} as a function of $1/T$) and the activation energy E_a was calculated from the slope ($-E_a/R$) of the regression lines, where R is the gas constant. Thermodynamic activation parameters at a fixed temperature were determined using the following equations (13),

$$\Delta G^{\ddagger} = RT \times (23.76 + \ln T - \ln k_{cat}) \text{ in J mol}^{-1} \quad \text{(Eq. 1)}$$

$$\Delta H^{\ddagger} = E_a - RT \quad \text{(Eq. 2)}$$

$$\Delta S^{\ddagger} = (\Delta H^{\ddagger} - \Delta G^{\ddagger})/T \quad \text{(Eq. 3)}$$

where $\Delta G^{\ddagger}$ is the free energy of activation, $\Delta H^{\ddagger}$ is the enthalpy, $\Delta S^{\ddagger}$ is the entropy of activation, and T is the temperature in degrees Kelvin.

Fluorescence Quenching—The flexibility of enzymes was estimated by acrylamide-induced fluorescence quenching at 351 nm. Samples were prepared in 30 mM MOPS, 50 mM NaCl, 1 mM $CaCl_2$, pH 7.2, and the final protein concentration was reduced to ±100 μg/ml to ensure that $A_{280} < 0.1$. Aliquots of an acrylamide stock solution (1.2 M) were consecutively added to 1 ml of the protein solution to increase acrylamide concentration by ~5 mM steps. Quenching data were plotted as the ratio of fluorescence in the absence of quencher (F_0) to the intensity in the presence of quencher (F) against quencher concentration. The calculated slope was equated to dynamic parameters according to the Stern-Volmer equation, $F/F_0 = 1 + K_{SV}[Q]$, where K_{SV} is the Stern-Volmer quenching constant and [Q] the concentration of quencher (21).

Differential Scanning Calorimetry—Measurements were performed using a MicroCal MCS-DSC instrument as detailed previously (14).

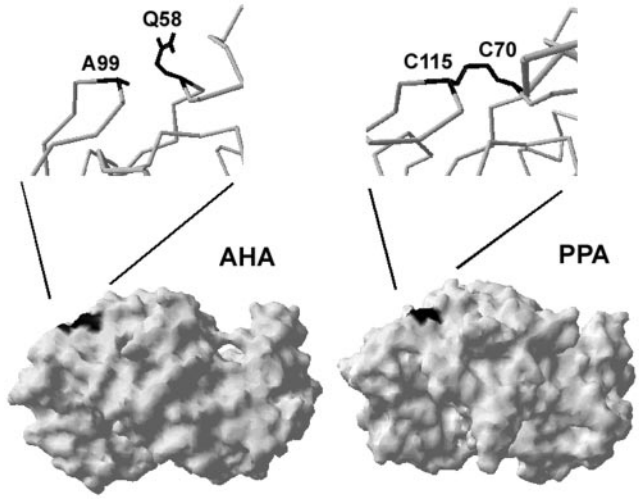

FIG. 1. **Structural comparison of AHA and PPA.** *Lower panel*, molecular surfaces of both enzymes with the two residues selected for mutagenesis in AHA in *black*. For PPA, the two corresponding cysteine residues are also *darkened*. *Upper panel*, structure of the disulfide bond in PPA and of the corresponding residues in AHA. The image was generated by SWISS-PDBVIEWER with atomic coordinates from 1AQH and 1PPI.

Samples (~3 mg/ml) were dialyzed overnight against 30 mM MOPS, 50 mM NaCl, 1 mM $CaCl_2$, pH 7.2. Thermograms were analyzed according to a non-two-state model in which T_m, ΔH_{cal}, and ΔH_{eff} of individual transitions are fitted independently using the MicroCal Origin software (version 2.9). The magnitude and source of the errors in the T_m and enthalpy values have been discussed elsewhere (22). Fitting standard errors on a series of three DSC measurements made under the same conditions in the present study were found to be ± 0.05 K on T_m and ± 1% on both enthalpies.

The stability curve of MutCC was calculated by summing the contributions of the calorimetric domains using the experimental ΔH_{cal} and T_m values, and ΔC_p values proportional to ΔH_{cal} (ΔC_p = 2.74 and 5.73 kcal mol^{-1} K^{-1}, respectively, for peaks 1 and 2) on the basis of ΔC_p = 8.47 kcal mol^{-1} K^{-1} determined for AHA (14).

Thermal Inactivation—Thermograms generated by starch enzymatic hydrolysis were recorded on a MCS Isothermal Titration Calorimeter (ITC). The technical background for such an experiment has been described elsewhere (23). Starch concentration was 2% in 50 mM HEPES, 50 mM NaCl, 1 mM $CaCl_2$, pH 7.2, and was saturating during the time course of the experiment. Reactions were initiated by injecting 10–50 μl of a 30 μg/ml enzyme solution in the same buffer. The activity decay at 45 °C was recorded continuously during 30 min, and data were fitted on a monoexponential function to determine the first order constant rate of enzyme inactivation at 45 °C; standard error on the mean was ≤1%.

RESULTS

Selection of Mutations—The mutations Q58C/A99C have been selected by comparing the primary and crystallographic structures of AHA and PPA (Fig. 1) (17, 24). In mammalian α-amylases, the disulfide bridge C58–C99 (AHA numbering) links domains A and B in the vicinity of the active site and is possibly responsible for the thermal stability of the activity of these enzymes (16, 17). Residues Gln-58 and Ala-99 in AHA, corresponding to cysteines in PPA, have the appropriate conformation to restore this bridge in the cold-active enzyme. The formation of the extra disulfide bridge in MutCC was confirmed by the absence of reaction with 5,5′-dithiobis-2-nitrobenzoic acid (25), because no other free cysteine occurs in AHA.

Kinetic Parameters—The kinetic parameters k_{cat} and K_m were recorded using a chromogenic maltoheptaose oligosaccharide at 5 and 25 °C (Table I). As expected for a cold-adapted enzyme, AHA possesses a higher specific activity than its mesophilic homologue PPA as well as a lower affinity for the substrate. The cross-link introduced in AHA induces signifi-

TABLE I
Kinetic parameters of wild-type and mutant α-amylases

	5 °C			25 °C		
	k_{cat}	K_m	k_{cat}/K_m	k_{cat}	K_m	k_{cat}/K_m
	s^{-1}	μM	$s^{-1}\ \mu M^{-1}$	s^{-1}	μM	$s^{-1}\ \mu M^{-1}$
AHA	293 ± 12	155 ± 6	1.89	697 ± 33	234 ± 18	2.98
MutCC	114 ± 6	71 ± 5	1.61	340 ± 13	112 ± 6	3.04
PPA	46 ± 4	25 ± 3	1.84	291 ± 8	65 ± 4	4.48

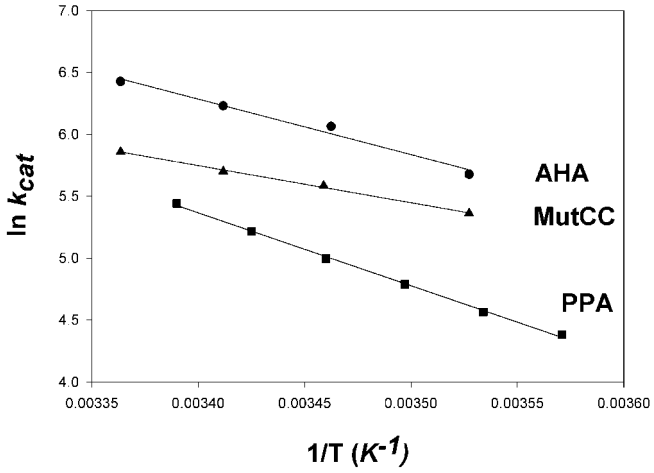

FIG. 2. **Arrhenius plots calculated from AHA, MutCC, and PPA activities.** MutCC activity is intermediate between AHA and PPA. The lower thermodependence of MutCC activity is reflected by the lower activation energy (E_a) derived from the slope of the regression line.

cant alterations of the kinetic parameters. Indeed, at 25 °C, MutCC exhibits a two times lower specific activity than AHA as well as a two times higher affinity for the substrate, therefore, approaching the mesophilic characteristics of PPA.

Activation Parameters—Specific activities were recorded between 5 and 25 °C (data not shown). From these results, two main aspects should be pointed out: (i) Activity of MutCC is intermediate between AHA and PPA activities at all temperatures (Table I) and (ii) the thermodependence curve of MutCC is flattened compared with that of psychrophilic and mesophilic wild-type enzymes. The lower thermodependence of MutCC activity is reflected by the lower activation energy, E_a, derived from Arrhenius plots (Fig. 2 and Table II). Activation parameters $\Delta G^{\ddagger}$, $\Delta H^{\ddagger}$, and $T\Delta S^{\ddagger}$ calculated at 15 °C are also presented in Table II. Although the activation free energy ($\Delta G^{\ddagger}$) for MutCC presents an intermediate value compared with AHA and PPA, the enthalpic ($\Delta H^{\ddagger}$) and entropic ($T\Delta S^{\ddagger}$) contributions are lower than the corresponding values of psychrophilic enzyme. Accordingly, despite a reduced thermodependence of the activity (low E_a and $\Delta H^{\ddagger}$), the intermediate rate constant k_{cat} (intermediate $\Delta G^{\ddagger}$) arises from an unfavorable entropic contribution.

Fluorescence Quenching—Fluorescence quenching is a dynamic process originating from the collision of a quencher (acrylamide) with a fluorophore (tryptophan residues) that induces a decreased intensity of the emitted fluorescence (21). This method was used to evaluate the structural flexibility of AHA and MutCC taking advantage of the presence of 12 Trp residues distributed throughout the psychrophilic protein: the higher the accessibility of the Trp residues for acrylamide, the larger the decrease of fluorescence intensity induced by a similar increase in quencher concentration. Data of fluorescence quenching at 5, 25, and 37 °C are presented in Fig. 3, and Stern-Volmer constants (K_{SV}) deduced from the slopes of the regression lines are given on Table III. These results demonstrate a lower quenching effect of acrylamide on MutCC at all temperatures, indicating a more rigid structure of the mutated α-amylase.

TABLE II
Kinetic and thermodynamic activation parameters at 15 °C for wild-type and mutant α-amylases

	k_{cat}	E_a	$\Delta G^{\ddagger}$	$\Delta H^{\ddagger}$	$T\Delta S^{\ddagger}$
	s^{-1}	*kcal mol*$^{-1}$			
AHA	388	8.9	13.4	8.3	−5.1
MutCC	252	5.9	13.7	5.4	−8.3
PPA	140	11.7	14.0	11.1	−2.9

Microcalorimetric Characterization—The thermal unfolding of AHA, PPA, and MutCC recorded by differential scanning calorimetry is illustrated in Fig. 4. As previously reported (14, 18), when compared with PPA, AHA is characterized by a lower melting point of unfolding (T_m), a lower calorimetric enthalpy (ΔH_{cal}) corresponding to the total amount of heat absorbed during unfolding, and a symmetric transition reflecting a two-state unfolding mechanism (Table IV). The extra disulfide bond significantly modifies the microcalorimetric pattern of MutCC, and two essential points are worth mentioning: (i) The calorimetric trace is no longer characteristic of a single transition but can be deconvoluted into two calorimetric units or domains. The lower T_m value of 40 °C for the first transition, compared with 44 °C for AHA, indicates that a calorimetric unit of the protein is somewhat disturbed by the engineered cross-link. (ii) By contrast, the total calorimetric enthalpy (ΔH_{cal}) has been increased from 214 to 241 kcal mol^{-1} for MutCC (Table IV), compared with the value of 295 kcal mol^{-1} for PPA, thus reflecting the global stabilizing effect of the extra disulfide bond as far as the enthalpic contribution is concerned. Considering the complete reversibility of AHA thermal unfolding and to determine thermal inactivation rate constants (k_{inact}), we recently proposed a new method using ITC and recording activity continuously (instead of classic residual activity measurements) at 45 °C as the heat released by the hydrolysis of starch glycosidic bonds (18). Using this method (data not shown), values of k_{inact} obtained for AHA, MutCC, and PPA were 2.27 10^{-3}, 4.46 10^{-3}, and 0 s^{-1}, respectively. Therefore, there is no significant inactivation of PPA at 45 °C, whereas the inactivation rate constant of MutCC is twice that of AHA.

DISCUSSION

Many previous studies have investigated the complex effects of additional disulfide bonds on proteins stability. Frequently however, added cross-links were purely artificial and predictions were based on examination of the three-dimensional structures, as exemplified by the barnase mutants (4–6). The specificity of mutant MutCC is that the additional cross-link introduced in AHA is actually present in its mesophilic homologues, therefore, reducing the probability of large structural modifications of the protein architecture. Other ectothermic species also possess a chloride-dependent amylase devoid of this particular bond. Accordingly, it is probably not fortuitous that all warm-blooded animals display heat-stable α-amylases containing this specific disulfide bond near the active site. The

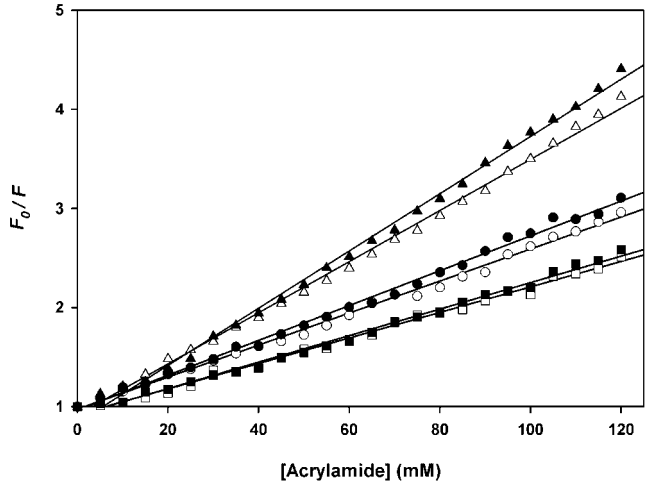

FIG. 3. **Fluorescence quenching by acrylamide.** The flexibility of AHA (*filled symbols*) and MutCC (*open symbols*) has been estimated by fluorescence quenching with acrylamide at 5 °C (*squares*), 25 °C (*circles*), and 37 °C (*triangles*). The slopes of the regression lines, corresponding to the Stern-Volmer constants (K_{SV}), are given in Table III.

TABLE III
Stem-Volmer quenching constants (K_{sv}) of wild-type AHA and of the disulfide bond mutant MutCC

	K_{sv}		
	5 °C	25 °C	37 °C
		$mM^{-1} \cdot 10^{-2}$	
AHA	1.34 ± 0.02	1.76 ± 0.02	2.89 ± 0.04
MutCC	1.29 ± 0.02	1.61 ± 0.02	2.58 ± 0.03

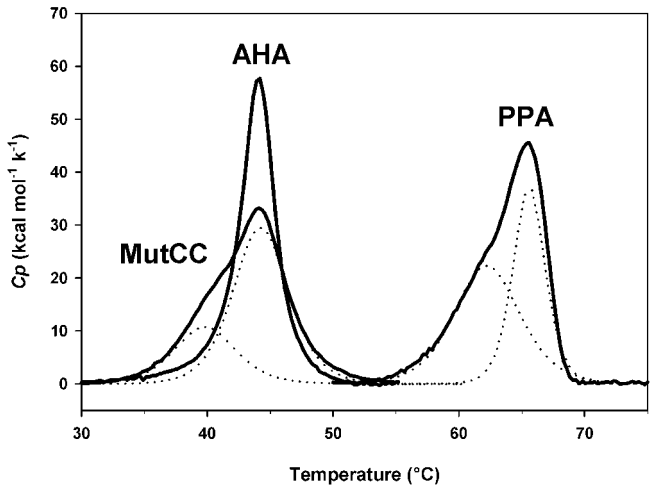

FIG. 4. **Thermal unfolding of α-amylases recorded by DSC.** Compared with AHA, PPA is characterized by a higher T_m (*top* of the transition) and ΔH_{cal} (*area under* the transition), and by the occurrence of calorimetric domains (deconvolutions are in *dotted lines*). MutCC has lost the typical two-state denaturation of AHA: the calorimetric trace includes two calorimetric domains and is characterized by a higher ΔH_{cal} value than AHA.

TABLE IV
Thermodynamic parameters of α-amylases unfolding recorded by microcalorimetry

	T_m	ΔH_{cal}	$\Sigma \Delta H_{cal}$
	°C	*kcal mol^{-1}*	
AHA	44.0	214	214
MutCC			
1[a]	40.0	78	
2	44.3	163	241
PPA			
1	61.7	147	
2	65.6	148	295

[a] 1 and 2 refer to calorimetric domains identified by deconvolution of DSC thermograms.

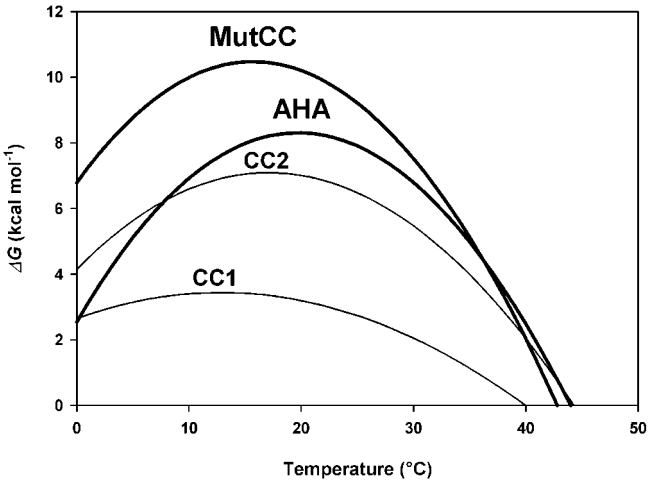

FIG. 5. **Stability curves of AHA and MutCC.** *CC1* and *CC2* represent the stability curves of the two calorimetric domains observed for MutCC (*thin lines*). Their sum provides the global stability curve for the mutant MutCC and demonstrates the stabilization induced by the engineered disulfide bond in comparison with wild-type AHA.

TABLE V
Thermodynamic parameters of conformational stability of wild-type AHA and of mutant MutCC at 20 °C

		ΔH	$T\Delta S$	ΔG
		kcal mol^{-1}		
AHA	1[a]	10.72	2.39	8.33
MutCC	1	23.16	19.97	3.19
	2	23.76	16.75	7.01
	1+2	46.92	36.72	10.20

[a] 1 and 2 refer to calorimetric domains identified by deconvolution of DSC thermograms.

engineered disulfide bond has a dual effect on the properties of the mutant enzyme: on the one hand, the protein is rigidified and its global stability is improved (as shown by fluorescence quenching and microcalorimetry), but on the other hand, strain has been introduced in the active site which consequently becomes less stable and heat-labile. Both aspects will be discussed separately.

Effect on Enzyme Activity—It is generally recognized that cold adaptation is achieved through an increased flexibility of the protein domain bearing the active site and responsible for its weak stability (10–12). The extra disulfide bond engineered in AHA rigidifies the surroundings of the cross-link, and it is striking that the catalytic parameters are significantly modified so that MutCC exhibits a lower k_{cat} as well as an improved K_m, approaching the values recorded for the pig enzyme (Table I). This correlation between catalytic parameters and localized mobility/rigidity is in agreement with a recent mutational study showing identical correlation when the protein is stabilized by weak non-covalent interactions (18).

Cold-active enzymes attenuate the inhibitory effect of low temperatures on activity by decreasing the temperature dependence of the catalyzed reaction, as demonstrated by their low activation energy (E_a) and activation enthalpy $\Delta H^{\ddagger}$ (13, 26). It has been proposed that the decreased $\Delta H^{\ddagger}$ value is structurally achieved by a decrease in the number of enthalpy-driven interactions that have to be broken during activation, leading to a heat-labile active site, because these interactions also

contribute to stability (13). The behavior of MutCC provides an experimental demonstration of this proposal. Indeed, strain has been imposed on the active site by the engineered disulfide bond, as indicated by the marked heat lability of the activity of MutCC. This increase of the thermal inactivation rate constant is accompanied by a strong reduction of the temperature dependence of the activity of MutCC, reflected by its low activation energy and activation enthalpy compared with the wild-type enzymes displaying a more stable activity (Fig. 2 and Table II). In addition, the activation entropy $\Delta S^{\ddagger}$ of MutCC is also larger than the values recorded for the wild-type enzymes (Table II). This alteration of $\Delta S^{\ddagger}$ possibly reflects that the ground-state enzyme-substrate complex *E*S occupies a broader distribution of conformational states, induced by the active site destabilization. Such variations of both $\Delta H^{\ddagger}$ and $\Delta S^{\ddagger}$ are in fact a general property of all heat-labile enzymes studied so far (13, 26), suggesting that the lower temperature dependence is indeed correlated to heat lability of activity. Finally, it should be stressed that the mutant MutCC displays two opposing properties: (i) alteration of the kinetic parameters k_{cat} and K_m toward values of heat-stable enzymes, which is possibly induced by global stabilization (discussed below) and (ii) alteration of the activation parameters toward values of heat-labile enzymes, which is possibly induced by active-site destabilization. This strongly suggests that both properties are not strictly physically linked in enzymes and is in agreement with directed evolution experiments showing that activity and stability can be altered independently, at least to some extent (27).

Effect of the Disulfide Bond on Protein Flexibility and Stability—The predominant effect of the new covalent bond on the α-amylase architecture is to bridge domains A and B forming the active site cleft at the domain interface (28, 29). The relative compactness of AHA and MutCC was estimated by fluorescence quenching and reveals a slightly more rigid structure for the mutant (Fig. 3). Indeed, fluorescence quenching is regarded as an index of protein permeability, because interactions of the quencher and fluorophores average the various protein motions in a large time scale (21). Although the differences in Stern-Volmer quenching constants are low at 5 °C, these differences significantly increase with temperature (Table III). It should be noted that 12 Trp residues are present in both proteins and can be quenched by acrylamide, however, only one is located close to the engineered disulfide bond. It should be stressed that the wild-type and mutant enzymes can be validly compared by this technique, because they are identical with the exception of the engineered bond.

As shown in Fig. 4, the extra disulfide bond results in the appearance of a small additional calorimetric domain and in a net increase of the calorimetric enthalpy ΔH_{cal} (Table IV). This additional domain displays a lower T_m value than the native enzyme, suggesting that it could be related to the active site domain as the inactivation rate constant of MutCC is increased. Because the unfolding of both calorimetric domains follow a reversible two-state mechanism, the thermodynamic stability can be analyzed using the modified Gibbs-Helmholtz equation,

$$\Delta G(T) = \Delta H_{cal}(1 - T/T_m) + \Delta C_p(T - T_m) - T\Delta C_p \ln (T/T_m) \quad \text{(Eq. 4)}$$

This function corresponds to the energy required to disrupt the native state (30) and has been calculated for both domains CC1 and CC2 (Fig. 5). The sum provides the global stability curve for MutCC, which is compared with the stability curve of AHA in Fig. 5. The general stabilizing effect of the extra disulfide bond is clearly demonstrated by the higher maximal ΔG value, which is increased by ~20% compared with AHA. The denaturation enthalpy and entropy can be calculated according to the relations (31),

$$\Delta H(T) = \Delta H_{cal} + \Delta C_p(T - T_m) \quad \text{(Eq. 5)}$$

$$\Delta S(T) = \Delta H_{cal}/T_m + \Delta C_p \ln (T/T_m) \quad \text{(Eq. 6)}$$

The calculated values at 20 °C are presented in Table V. For instance, the gain of 1.87 kcal/mol in conformational energy provided by the cross-link at 20 °C arises from a 4.4-fold increase of the denaturation enthalpy balanced by a 15.4-fold increase of the entropic cost. It is clear from these results that the cross-link stabilizes the enzyme enthalpically but destabilizes it entropically, thereby lowering the net gain in free energy of conformational stability. This enthalpy-entropy compensation effect probably explains the difficulty of strongly stabilizing a protein by introducing an extra disulfide bond. In contrast with the results obtained for trypsin inhibitor-V (8), our results are in agreement with the Doig and Williams model (2), although it must be kept in mind that this theory does not consider the effects of the disulfide bond on the native state. In contrast, it is generally recognized that effects on both native and unfolded states of proteins must be considered. The fluorescence quenching experiments strongly suggest that the newly introduced cross-link has rigidified the native state of the enzyme, in particular near the catalytic domain where it is located. This should result in a decreased entropy of the folded state structure and therefore should be partly responsible for the increase in denaturation entropy calculated in Table V. Interestingly, the value obtained for the first transition (possibly corresponding to the catalytic domain) is actually higher.

CONCLUSION

The extra disulfide bond has paradoxical effects on the intrinsic properties of the enzyme. In most cases, bridging domains A and B of the protein structure near the catalytic site, as in heat-stable α-amylases, resulted in a mesophilic-like entity supported by (i) the modified catalytic parameters, (ii) the rigidified protein structure, and (iii) the enthalpy-driven stabilization of the folded state of the protein. However, the strain imposed on this particular site is not compensated for in other protein regions as is probably the case for heat-stable enzymes. This resulted in a slightly perturbed architecture revealed by the thermodynamic activation parameters and DSC and ITC experiments. This study demonstrates the difficulty in increasing protein stability by simply adding an extra cross-link in a large protein. In addition, it supports the subtle variations that a cross-link can induce in an enzyme or a protein in general to allow specific environmental adaptations.

Acknowledgments—We thank N. Gérardin and R. Marchand for their skillful technical assistance. We also thank D. Georlette, T. Collins, and J.-C. Marx for helpful assistance and discussions. The generous support of the Institut Polaire Français is also highly appreciated.

REFERENCES

1. Pace, C. N., Grimsley, G. R., Thomson, J. A., and Barnett, B. J. (1988) *J. Biol. Chem.* **263,** 11820–11825
2. Doig, A. J., and Williams, D. H. (1991) *J. Mol. Biol.* **217,** 389–398
3. Betz, S. F. (1993) *Protein Sci.* **2,** 1551–1558
4. Clarke, J., Henrick, K., and Fersht, A. R. (1995) *J. Mol. Biol.* **253,** 493–504
5. Clarke, J., Hounslow, A. M., and Fersht, A. R. (1995) *J. Mol. Biol.* **253,** 505–513
6. Johnson, C. M., Oliveberg, M., Clarke, J., and Fersht, A. R. (1997) *J. Mol. Biol.* **268,** 198–208
7. Vogl, T., Brengelmann, R., Hinz, H. J., Scharf, M., Lotzbeyer, M., and Engels, J. W. (1995) *J. Mol. Biol.* **254,** 481–496
8. Zavodszky, M., Chen, C. W., Huang, J. K., Zolkiewski, M., Wen, L., and Krishnamoorthi, R. (2001) *Protein Sci.* **10,** 149–160
9. D'Amico, S., Gerday, C., and Feller, G. (2000) *Gene* (*Amst.*) **253,** 95–105
10. Zavodszky, P., Kardos, J., Svingor, and Petsko, G. A. (1998) *Proc. Natl. Acad. Sci. U. S. A.* **95,** 7406–7411
11. Zecchinon, L., Claverie, P., Collins, T., D'Amico, S., Delille, D., Feller, G., Georlette, D., Gratia, E., Hoyoux, A., Meuwis, M. A., Sonan, G., and Gerday, C. (2001) *Extremophiles* **5,** 313–321
12. D'Amico, S., Claverie, P., Collins, T., Georlette, D., Gratia, E., Hoyoux, A.,

Meuwis, M. A., Feller, G., and Gerday, C. (2002) *Phil. Trans. R. Soc. Lond. B* **357,** 917–925
13. Lonhienne, T., Gerday, C., and Feller, G. (2000) *Biochim. Biophys. Acta* **1543,** 1–10
14. Feller, G., d'Amico, D., and Gerday, C. (1999) *Biochemistry* **38,** 4613–4619
15. Kumar, S., Tsai, C. J., and Nussinov, R. (2002) *Biochemistry* **41,** 5359–5374
16. Aghajari, N., Feller, G., Gerday, C., and Haser, R. (1998) *Structure* **6,** 1503–1516
17. Aghajari, N., Feller, G., Gerday, C., and Haser, R. (1998) *Protein Sci.* **7,** 564–572
18. D'Amico, S., Gerday, C., and Feller, G. (2001) *J. Biol. Chem.* **276,** 25791–25796
19. Feller, G., le Bussy, O., Houssier, C., and Gerday, C. (1996) *J. Biol. Chem.* **271,** 23836–23841
20. Feller, G., le Bussy, O., and Gerday, C. (1998) *Appl. Environ. Microbiol.* **64,** 1163–1165
21. Lakowicz, J. (1983) *Principles of Fluorescence Spectroscopy*, pp. 257–301, Plenum Press, New York
22. Matouschek, A., Matthews, J. M., Johnson, C. M., and Fersht, A. R. (1994) *Protein Eng.* **7,** 1089–1095
23. Lonhienne, T., Baise, E., Feller, G., Bouriotis, V., and Gerday, C. (2001) *Biochim. Biophys. Acta* **1545,** 349–356
24. Qian, M., Haser, R., Buisson, G., Duee, E., and Payan, F. (1994) *Biochemistry* **33,** 6284–6294
25. Sedlak, J., and Lindsay, R. H. (1968) *Anal. Biochem.* **25,** 192–205
26. Low, P. S., Bada, J. L., and Somero, G. N. (1973) *Proc. Natl. Acad. Sci. U. S. A.* **70,** 430–432
27. Wintrode, P. L., and Arnold, F. H. (2000) *Adv. Protein Chem.* **55,** 161–225
28. Qian, M., Haser, R., and Payan, F. (1993) *J. Mol. Biol.* **231,** 785–799
29. Larson, S. B., Greenwood, A., Cascio, D., Day, J., and McPherson, A. (1994) *J. Mol. Biol.* **235,** 1560–1584
30. Privalov, P. (1992) in *Protein Folding* (Creighton, T., ed) pp. 83–126, W. H. Freeman and Company, New York
31. Privalov, P. L. (1979) *Adv. Protein Chem.* **33,** 167–241